Journal of Macromolecular Science, Part A: Pure and Applied Chemistry
Publication details, including instructions for authors and subscription information:
http://www.tandfonline.com/loi/lmsa20

# Direct-write, Well-aligned Chitosan-Poly(ethylene oxide) Nanofibers Deposited via Near-field Electrospinning

Yiin-Kuen Fuh [a], Shengzhan Chen [a] & Jason S.C. Jang [a b]
[a] Department of Mechanical Engineering, National Central University, Taoyuan County, Taiwan
[b] Institute of Materials Science and Engineering, National Central University, Taoyuan County, Taiwan
Published online: 12 Sep 2012.

To cite this article: Yiin-Kuen Fuh, Shengzhan Chen & Jason S.C. Jang (2012) Direct-write, Well-aligned Chitosan-Poly(ethylene oxide) Nanofibers Deposited via Near-field Electrospinning, Journal of Macromolecular Science, Part A: Pure and Applied Chemistry, 49:10, 845-850, DOI: 10.1080/10601325.2012.714676

To link to this article: http://dx.doi.org/10.1080/10601325.2012.714676

*Journal of Macromolecular Science, Part A : Pure and Applied Chemistry* (2012) **49**, 845–850

ISSN: 1060-1325 print / 1520-5738 online
DOI: 10.1080/10601325.2012.714676

Taylor & Francis
Taylor & Francis Group

# Direct-write, Well-aligned Chitosan-Poly(ethylene oxide) Nanofibers Deposited via Near-field Electrospinning

YIIN-KUEN FUH[1]*, SHENGZHAN CHEN[1], and JASON S.C. JANG[1,2]

[1]*Department of Mechanical Engineering, National Central University, Taoyuan County, Taiwan*
[2]*Institute of Materials Science and Engineering, National Central University, Taoyuan County, Taiwan*

Received March 2012, Accepted May 2012



A continuous near-field electrospinning (NFES) process has been demonstrated to be able to achieve direct-write and well-aligned chitosan/poly(ethylene oxide) nanofibers. The ability to precisely control and deposit chitosan-based nanofibers in a direct-write manner is favorable in manipulating cells attachment and proliferation at a preferred position. Experimental results show that fiber diameters can be reliably controlled in the range of 265–1255 nm by adjusting various operating parameters of the NFES processes. These prescribed patterns of nanofibers exceed tens of centimeters long and complex configurations such as grid arrays and arc shapes are assembled at specified separations as small as 5 $\mu$m. FTIR analysis reveals that NFES nanofibers have a similar morphology and composition as conventional electrospinning counterpart and constitute all components formerly present in the polymer solution. The versatile functionality to fabricate chitosan-based nanofibers with controllable size and directional alignment as well as highly ordered and customized patterns may represent an ideal candidate of a functional biomaterial and in tissue-engineering scaffolds that are predominantly representative of extracellular matrix (ECM).

**Keywords:** Well-aligned, chitosan-poly(ethylene oxide), nanofibers, near-field electrospinning

## 1 Introduction

Nanoscale polymer fibers can be fabricated in a simple and inexpensive manner via electrospinning processes. Conventionally, nanofibers are suitable for a wide spectrum of applications such as texturing and tissue scaffolds (1, 2). Electrospinning has been widely recognized as an efficient technique for the fabrication of polymer nanofibers. In parallel, a comprehensive review of electrospinning has been also presented on the processing, structure and property characterization, applications, and modeling and simulations related to electrospun polymer nanofibers (3). In the conventional electrospinning process, a Taylor cone is induced due to sufficient electrostatic forces to electrically charge and deform the polymer meniscus into a conical shape. At the tip of Taylor cone, a critical electrical field to induce a polymer jet is characterized experimentally at which electrostatic forces overcome the surface tension forces (4). However, the chaotic nature of conventional electrospinning process will result in instability of polymer jet and deposit nanofibers in a disorder and random fashion (5). How to develop orderly electrospinning processes still pose a severe challenges in terms of practicality and dynamic mechanical devices such as use of a rotating shaft, which has been shown to be promising but lacks position (6, 7). Continuous near-field electrospinning was recently developed as a favorable technology due to easier and predictable location control for the deposition of nanofibers. Fundamentally, when the needle-to-collector distance implemented Figure 1(a) a significant reduction from several centimeters to few millimeters, the applied bias voltage can also be reduced to few hundreds of volts. In addition, collector substrate is typically placed onto a programmable x-y stage to facilitate the deposition of direct-write and well-ordered nanofibers (8–10).

It is of great interest in tissue engineering to use polymeric nanofibers as scaffolding materials (11). In particular, the natural extracellular matrix (ECM) as a biomimic materials which allows cells to attach and proliferate and the morphology can be substantially engineered through material size features (12, 13). Chitosan has been widely studied due to its unique properties such as naturally nontoxic, biodegradable and anti-microbial (14). Structurally, chitosan is a copolymer of N-acetyl-Dglucosamine and D-glucosamine (15, 16). In the previous report, chitosan solutions blended with poly(ethylene oxide) (PEO) and poly(vinyl alcohol) (PVA) have been successfully Figure 2 electrospun (17) via a conventional electrospinning process. For biomedical applications, PEO is widely used due

*Address correspondence to: Yiin-Kuen Fuh, Department of Mechanical Engineering, National Central University, Taoyuan County 32001, Taiwan. Email: mikefuh@ncu.edu.tw

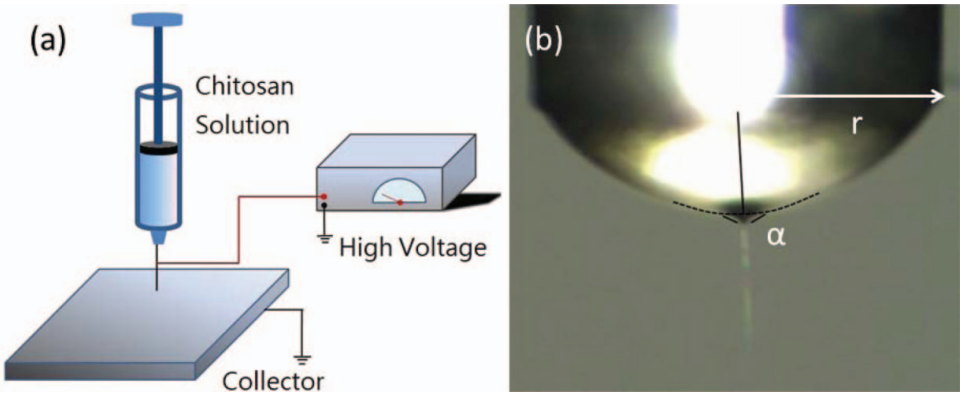


**Fig. 1.** (a) Schematic view of the experimental setup using NFES process, (b) The syringe needle radius r = 200 $\mu$m, droplet, and Taylor cone $\alpha = 63^\circ$ in near-field setup where applied voltage is 1.0 kV and needle-to-collector distance is 500 $\mu$m. (Color figure available online.)



to reduced toxicity concerns and enhanced biocompatibility of the nanofibrous membranes. In addition, PEO shows excellent electrospinning characteristics such as plasticizer-like behavior to facilitate orientation, ability to form ultrafine fibers, linear structure with flexible chains, solubility in aqueous media, and capabale to form hydrogen bonds with other macromolecules (18, 19). In this work, we present the experimental results of direct-write and addressable deposition of nanofibers in a contiunous fashion via NFES and well-aligned chitosan/PEO nanofibers are investigated by means of optical microscope (OM), scanning electron microscope (SEM) and Fourier transform infrared spectroscopy (FTIR).

## 2. Experimental

### 2.1 Materials

Chitosan from crab shells with 85% of deacetylation (Mw = 190 kD) was purchased from Sigma Chemical Co. Poly(ethylene oxide) (PEO) (Mw = 900 kD), Triton X-100$^{TM}$, were provided by Across Co, and dimethylsulphoxide (DMSO) was obtained from Tedia Co. All reagents were used as received from the manufacturer without further purification.

### 2.2 Preparation of Stock Solutions for Electrospinning

4% chitosan solution and 5% PEO solution were first prepared separately by dissolving chitosan in 0.5M acetic acid, followed by oven vacuum at 0.8 torr to remove air bubbles. Then the mixtures with weight ratios of chitosan to PEO were prepared ranging from 90/10 to 50/50 and magnetically stirred for 5 h. Solutions containing 0.5 wt% of Triton X-100$^{TM}$ and 5–10 wt% of DMSO were mixed with chitosan/PEO solutions, and the mixtures were again stirred for 16 h and vacuumed to remove air bubbles before use.

### 2.3 Electrospinning of Nanofibers

The stock solution for electrospinning was fed into a 1ml disposable syringe fitted with a needle tip of 0.4 mm in diameter, the applied electrostatic voltage was about 0.6–1.2 kV (AU-1592, Matsusada Precisioninc, JP.), the distance between the syringe tip and the grounded collector was 500–1500 $\mu$m. The substrate was mounted onto the programmable x-y stage (Yokogawa Inc.), controlled by a personal computer, which allows the movement of the sample during the nanofiber deposition. A polymer feed rate of about 0.1uL/h is used due to the reason that a steady droplet shape can be maintained for continuous and uniform deposition of nanofibers. The experiment was carried out at room temperature and atmospheric pressure. FTIR studies were carried out using a FTIR spectrophotometer (Jasco FTIR-410, JP) on electrospinning nanofibers containing KBr pellets (23). NFES chitosan-PEO nanofibers were electrospun a dozen of times (typically 10–20 patterns in dimension of 40 mm × 40 mm substrate) and mixed with KBr (the mass ratio of the sample/KBr was 1/100). Then a translucent pellet for FTIR analysis is obtained by crushing and finely grinding in a mechanical die press as described previously (26).

## 3. Results and Discussion

### 3.1 Electrospinning

The schematic of the NFES experimental setup is shown in Figure 1(a). Figure 1(b) shows the formation of Taylor cone under an optical microscope during the NFES process. The outer diameter of syringe needle is 400 $\mu$m, the distance of needle-to-collector is 500 $\mu$m, and the mixture of 90/10 chitosan/PEO is used in this case. The cone has a semi-vertical angle of around 63° while the applied voltage is maintained at 1.0 kV with the aid of initial mechanical drawing process. On the other hand, for pure PEO solution

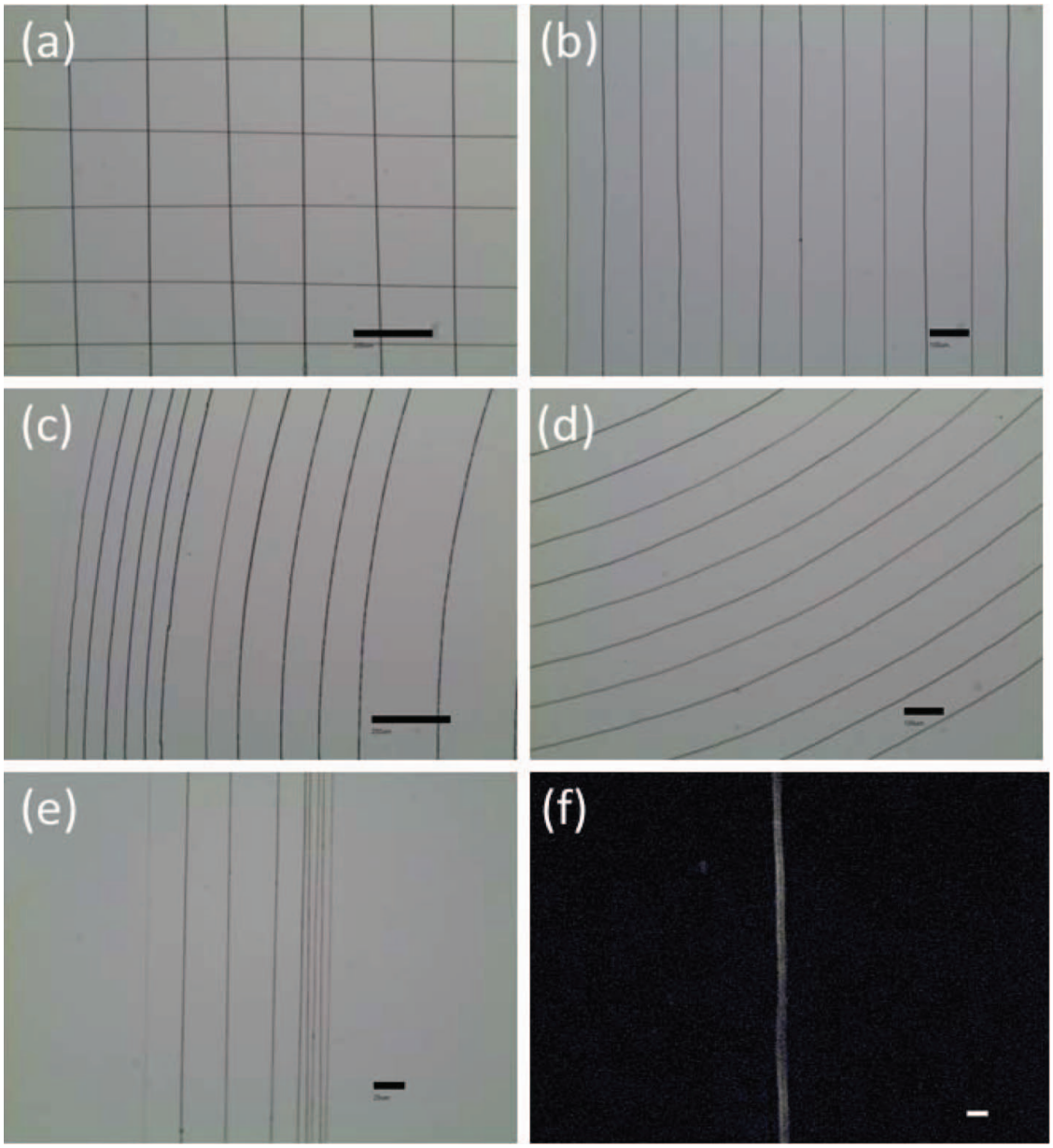


**Fig. 2.** Experiments showing controllability of NEFS for chitosan/PEO fibers. (a) A grid pattern with controlled 200 $\mu$m spacing, (b) Parallel fibers with controlled 100 $\mu$m spacing, (c) Arc pattern with controlled and incremental spacings of 50, 100, 200 $\mu$m, respectively, (d) Arc pattern with controlled 100 $\mu$m spacing, (e) Parallel fibers with controlled 5, 10, 20 $\mu$m spacing, respectively, (f) A single electrospun chitosan/PEO nanofiber with diameter of 350 nm. The scale bars for (a) and (d) are 200 $\mu$m; (b) and (c) are 100 $\mu$m; (e) is 20 $\mu$m; (f) is 500 nm. (Color figure available online.)

in near-field setup, the cone has a 49° semi-vertical angle and the applied votage is maintained at 1.5kV. Using reduced voltage of 0.6kV and the initial mechanical drawing process, when semi-vertical angle is increased to 75°, the drastically smaller nanofibers can be obtained (8).

Figure 2(a–f) show the OM and SEM images of chitosan parallel nanofibers constructed using a programmable x-y stage. The collector movement can be controlled with a speed of 20 cm/s and applied voltage of 0.8 kV. The chitosan/PEO complex is in 50/50 weight ratio and the needle-to-collector distance is 500 $\mu$m. In Figure 2(a–b), the nanofibers can be assembled into controlled and prescribed patterns such as parallel and grid arrays at specified distance of 100 and 200 $\mu$m, respectively. In addition, Figure 2(c) shows nanofibers at incremental spacings of 50, 100, 200 $\mu$m, respectively and Figure 2(d) demonstrates multiple arc shapes with center radius of 4000 $\mu$m and separation increment of 100 $\mu$m. In order to find applications of NFES precise deposition and directional alignment, chitosan-based nanofibers to form nonwoven mats

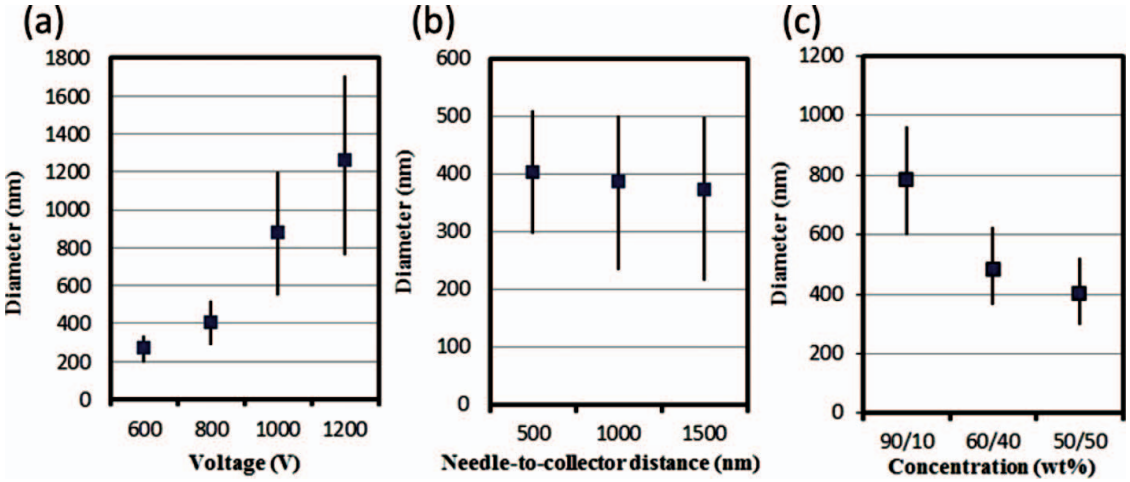


**Fig. 3.** Plots showing the dependence of nanofiber diameters on various processing parameters. (a) Applied voltage. Other parameters are maintained as the following: chitosan/PEO weight ratios is 50/50 and needle-to-collector distance 500 $\mu$m, (b) Needle-to-collector distance. Other parameters are maintained as the following: chitosan/PEO weight ratios is 50/50 and applied voltage 0.8 kV, (c) Polymer concentration. Other parameters are maintained as the following: applied voltage 0.8 kV and needle-to-collector distance 500 $\mu$m. All experiments are under room temperature and 1 atm pressure. (Color figure available online.)



or 2D porous structures open up a great opportunity of natural polymer-based ECMs (13). Therefore, the nanofibers distance was intentionally adjusted to be 5 $\mu$m, 10 $\mu$m, 20 $\mu$m, respectively (as shown in Fig. 2(e)) to facilitate possible experiments such as cells attachment, proliferation and migration. Meanwhile, a single electrospun chitosan/PEO nanofiber with diameter of 350 nm also can be made by NFES process as shown in Figure 2(f). Continuous depositions of chitosan/PEO mixture are also demonstrated that the smoothness Figure 3(a) of the pattern can be achieved by minimizing the difference between the translational speed of the stage and deposition rate. Regardless of the intricacy of the pattern, the criteria of equalizing the speed of the x-y stage and the electrospinning deposition rate is essential for smoothness of NFES processes.

In the continuous NFES process, the diameter of nanofibers can be repeatedly adjusted through various operating parameters such as applied voltage, needle-to-collector distance and weight ratios of solution (8). The following characterization of fiber diameters and standard deviations are calculated based on 50 data points measured directly from SEM in each experiment. When the chitosan/PEO complex is in 50/50 weight ratio, under different applied voltages, and the needle-to-collector distance is fixed at 500 $\mu$m, the average fiber diameter can be varied in the range of 266 $\pm$ 61 to 1290 $\pm$ 252 nm as shown in Figure 3(a). The proportional relationship of higher voltage results in thicker fibers in continuous NFES is also demonstrated in our experiment using chitosan/PEO solution. This effect is explained previously such that the initial polymer jet diameter dominates the final nanofiber diameter rather than bending instability at short needle-to-collector distance (8). Conversely, larger needle-to-collector distance results in thinner fibers (as shown in Fig. 3(b)) and the reason can be attributed to a longer travel period of polymer jets stretching, and the average fiber diameter ranges from 402 $\pm$ 85 to 373 $\pm$ 103 nm when the applied voltage is 0.8 kV and the chitosan/PEO complex in 50/50 weight ratios. As shown in Figure 3(c), when the needle-to-collector distance is fixed at 500 $\mu$m under a bias voltage of 0.8 kV, the average fiber diameter exhibits a decreasing trend from 787 $\pm$ 120 to 402 $\pm$ 85 nm by decreasing the chitosan/PEO weight ratio from 90/10 to 50/50. The reason is suggested due to the solution viscosity, which the spinnability and morphology of as-spun fibers are directly related to chitosan/PEO weight ratio (3, 20). Previously, different weight ratios of chitosan/PEO mixtures had been performed to investigate the relationship between shear viscosity and shear rate. It has been demonstrated that viscosity decreases with increased addition of PEO and so as to form thinner nanofibers (13).

### 3.2 Study of Fourier Transform Infrared Spectroscopy

For the samples of pure chitosan shown in Figure 4, curve e (which could not be electrospun (18)) typically displays characteristic absorption bands at 3400–3100 $cm^{-1}$ which are found to be attributed to N–H and OH/O stretching vibrations and intermolecular hydrogen bonding of the polysaccharide molecules (18, 21). In our measurement, N–H and OH/O absorption bands are found at 3400 $cm^{-1}$. In addition, previous research reported that carbonyl C=O–NHR or amide I band and the amine $–NH_2$ or amide II absorption band are 1680 and 1538 $cm^{-1}$, respectively (22). NFES samples also display similar characteristics which both carbonyl C=O–NHR and the amine $–NH_2$ absorption band are found at 1680 and 1540 $cm^{-1}$, respectively. Three peaks at 1380, 1316, and 1255 $cm^{-1}$

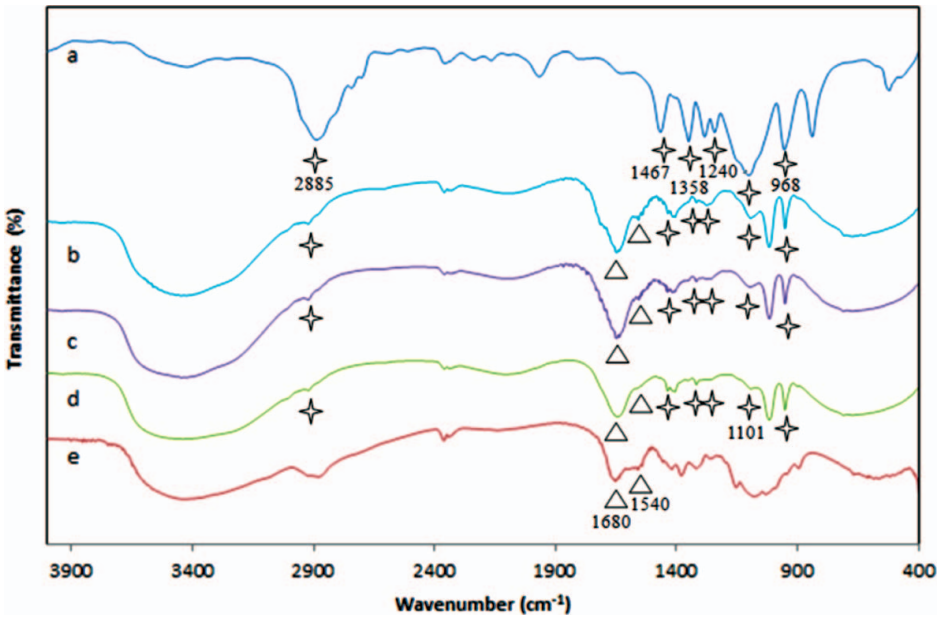


**Fig. 4.** FTIR spectra of chitosan and PEO and chitosan/PEO complex. PEO (a) and chitosan (e); chitosan/PEO complex in different mass ratios, (b) 90/10; (c) 60/40; (d) 50/50. The peaks labeled ' ☆'indicate the presence of chitosan and the peaks labeled '△' indicate the presence of PEO. (Color figure available online.)

assigned to the deformation of C–$CH_3$ and the amide III band. In our measurement, C–$CH_3$ and the amide III band absorption band are found at 1380, 1320, and 1255 $cm^{-1}$. As to the chitosan/PEO mixed solutions with various compositions shown in curves b-d of Figure 4, the triplet peaks of the C-O-C stretching vibrations appeared at 1148,1101 and 1062 $cm^{-1}$ with a maximum at 1101 $cm^{-1}$ (18). This is in good agreement with our measurement, the peaks of the C-O-C stretching vibrations appeared with a maximum at 1101 $cm^{-1}$, and at 1467 $cm^{-1}$ assigned to CH bending, at 1358 and 1340 $cm^{-1}$ assigned to CH deformation of the methyl group. The OH absorption bands can be neglected in current experimental setup due to a relatively high molecular weight (900 kDa) of PEO in this experiment (24). FTIR also shows the OH absorption bands at 3400 and 3100 $cm^{-1}$ and this may be attributed to stretching vibrations within the chitosan polysaccharide chains (24). Another trend is also observed that the absorbance intensity of $CH_2$ stretching at 2885 $cm^{-1}$ increased with the addition of PEO (25). Moreover, the $CH_2$ absorption band of our measurement is found at 2885 $cm^{-1}$ for NFES samples, and demonstrates that NFES electrospun chitosan/PEO nanofibers are similar to conventional electrospinning in terms of molecular structures and compositions. No significant shifts were observed in major absorption peaks and electrospun nanofibers are compositionally consistent with original solution. This is a good indication of a successful electrospinning process such that no component was selectively excluded during the electrospinning (18). It is concluded that NFES nanofibrous membranes should be able to meet cellular compatibility and apply to advanced studies of cell adhesion, spreading and interaction.

## 4 Conclusions

In summary, a continuous NFES technique is applied successfully to assemble direct-write, well-aligned chitosan/poly(ethylene oxide) nanofibers that are difficult to achieve by conventional electrospinning. Moreover, the nanofibers with a typical diameter of 350 nm can be deposited continuously and the complex patterns are assembled by controlling both NFES processing parameters such as applied electric field and solution concentration as well as the movement of the collector using a programmable x–y stage. Furthermore, the compositional analysis by FTIR reveals that NFES nanofibers have a similar morphology and composition as compared to counterparts using conventional electrospinning. Despite of the significant differences in both NFES and conventional processes such as electrical fields and evaporation time, the molecular interactions characterized by FTIR reveal strikingly resemblances in characteristic absorption bands from 400 to 4000 $cm^{-1}$ for the groups of N–H, OH/O, C=O–NHR, –$NH_2$, C-O-C, CH, OH and $CH_2$. No significant shifts were observed in major absorption peaks, except for variations in the intensity of some bands. It is believed that NFES will become an indispensable technology in generating 2D and prescribed patterned nanostructures to mimic the native extracellular matrix for tissue engineering.

## References

1. Pawlowski, K.J., Belvin, H.L., Raney, D.L., Su, J., and Harrison, E.J. (2003) *Polymer*, 44, 1309–1314.

2. Yeo, I.S., Oh, J.E., Jeong, L., Lee, T.S., Lee, S.J., Park, W.H., and Min, B.M. (2008) *Biomacromolecules*, 9, 1106–1116.
3. Huang, Z.M., Zhang, Y.Z., Kotaki, M., and Ramakrishna, S. (2003) *Composites Science and Technology*, 63, 2223–2253.
4. Sun, D., Chang, C., Li, S., and Lin, L. (2006) *Nanoletters*, 6(4), 839–842.
5. Schiffman, J.D., and Schauer, C.L. (2007) *Biomacromolecules*, 8, 2665–2667.
6. Matthews, J.A., Wnek, G.E., Simpson, D.G., and Bowlin, G.L. (2002) *Biomacromolecules*, 3, 232–238.
7. Katta, P., Alessandro, M., Ramsier, R.D., and Chase, G.G. (2004) *Nanoletters*, 4(11), 2215–2218.
8. Chang, C., Limkrailassiri, K., and Lin, L. (2008) *Applied Physics Letters*, 93, 123111.
9. Rinaldi, M., Ruggieri, F., Lozzi, L., Santucci, S., and Vac, J. (2009) *Sci. Technol. B*, 27(4), 1829–1833.
10. Carnell, L.S., Siochi, E.J., Wincheski, R.A., Holloway, N.M., and Clark, R.L. (2009) *Scripta Materialia*, 60, 359–361.
11. Caracciolo, P.C., Thomas, V., Vohra, Y.K., Buffa, F., and Abraham, G.A. (2009) *J. Mater. Sci. Mater. Med.*, 20, 2129–2137.
12. Li, W.J., Tuli, R., Okafor, C., Derfoul, A., Danielson, K.G., Hall, D.J., and Tuan, R.S. (2005) *Biomaterials*, 26, 599–609.
13. Bhattarai, N., Edmondson, D., Veiseh, O., Matsen, F.A., and Zhang, M. (2005) *Biomaterials*, 26, 6176–6184.
14. Desai, K., and Kit, K. (2008) *Polymer*, 49, 4046–4050.
15. Giner, S.T., Ocio, M.J., and Lagaron, J.M. (2008) *Eng. Life Sci.*, 8(3), 303–314.
16. Li, L., and Hsieh, Y.L. (2006) *Carbohydrate Research*, 341, 374–381.
17. Zhang, Y.Z., Su, B., Ramakrishna, S., and Lim, C.T. (2008) *Biomacromolecules*, 9, 136–141.
18. Kriegel, C., Kit, K.M., McClements, D.J., and Weiss, J. (2009) *Polymer*, 50, 189–200.
19. Han, J., Zhang, J., Yin, R., Ma, G., Yang, D., and Nie, J. (2011) *Carbohydrate Polymers*, 83, 270–276.
20. Reneker, D.H., and Chun, I. (1996) *Nanotechnology*, 7, 216–223.
21. Min, B.M., Lee, S.W., Lim, J.N., You, Y., Lee, T.S., Kang, P.H., and Park, W.H. (2004) *Polymer*, 45, 7137–7142.
22. Haider, S., Al-Masry, W.A., Bukhari, N., and Javid, M. (2010) *Polymer Engineering and Science*, 10, 1887–1893.
23. Chen, Z., Mo, X., and Qing, F. (2007) *Materials Letters*, 61, 3490–3494.
24. Sawatari, C., and Kondo, T. (1999) *Macromolecules*, 32(6), 1949–1955.
25. Duan, B., Dong, C.H., Yuan, X.Y., and Yao, K.D. (2004) *J. Biomat. Sci.-Polym. E*, 15, 797–811.
26. Homa, H., Seyed, A.H.R., and Masoumeh V. (2009) *Carbohydrate Polymers*, 77, 656–661.